

A LATITUDE-DEPENDENT WIND MODEL FOR MIRA'S COMETARY HEAD

A. C. RAGA¹, J. CANTÓ², F. DE COLLE³, A. ESQUIVEL¹, P. KAJDIC⁴, A. RODRÍGUEZ-GONZÁLEZ¹, P. F. VELÁZQUEZ¹

Accepted for publication in ApJL

ABSTRACT

We present a 3D numerical simulation of the recently discovered cometary structure produced as Mira travels through the galactic ISM. In our simulation, we consider that Mira ejects a steady, latitude-dependent wind, which interacts with a homogeneous, streaming environment. The axisymmetry of the problem is broken by the lack of alignment between the direction of the relative motion of the environment and the polar axis of the latitude-dependent wind. With this model, we are able to produce a cometary head with a “double bow shock” which agrees well with the structure of the head of Mira’s comet. We therefore conclude that a time-dependence in the ejected wind is not required for reproducing the observed double bow shock.

Subject headings: circumstellar matter – hydrodynamics – stars: AGB and post-AGB – stars: individual (Mira) – ISM: jets and outflows

1. INTRODUCTION

Martin et al. (2007) describe UV observations of a cometary structure extending over 2° in the sky, with its head centered on Mira. These observations were carried out with the GALEX satellite, with a filter with a central wavelength $\lambda_c = 1516 \text{ \AA}$ and a FWHM $\Delta\lambda = 256 \text{ \AA}$. Martin et al. (2007) speculate that part of the observed emission could be associated with the fluorescent UV lines of the H₂ molecule. Also, part of the emission (particularly in the head of the cometary structure) could correspond to emission from ionized species (e. g., from C IV) with lines which fall in the bandwidth of the filter. We present a schematic diagram of the UV image of Mira’s comet of Martin et al. (2007) in Figure 1.

Mira is a binary system with an AGB star and a less luminous companion which is probably a white dwarf. The binary system moves through the plane of the galaxy with a spatial velocity of $\approx 130 \text{ km s}^{-1}$, at an orientation of $\approx 30^\circ$ with respect to the plane of the sky, as can be deduced from the proper motion (Turon et al. 1993), radial velocity (Evans 1967) and Hipparcos-based distance (107 pc, Knapp et al. 2003). The proper motion is directed at an angle of 187° (measured E from N, see Wareing et al. 2007).

Wareing et al. (2007) computed a 3D simulation, in which they model this object as the interaction between an isotropic wind from the asymptotic giant branch (AGB) primary star and a streaming, homogeneous medium. Their simulation produces structures which are similar to the observed cometary structure. However, it is clear that the predicted flow does not show the detailed structure of condensations observed in the head of Mira’s comet (see Figure 3 of Martin et al. 2007).

In the present paper we explore whether or not the

“double bow shock” structure of the head of Mira’s comet can be reproduced by a somewhat more complex model. In modelling the structures of planetary nebulae (PNe), it is quite common to consider that the wind from AGB stars has a strong, equatorial density enhancement. Such a latitude-dependent wind can be used for reproducing the structures of many observed PNe and Proto-PNe (see, e.g., Balick & Frank 2002).

In the case of Mira, we could also be seeing the interaction of a latitude-dependent wind with an environment which sweeps past the source. We have, however, few constraints of the characteristics and orientation of this latitude-dependent wind. The only real observational constraint is that the Mira binary system has an orbital plane that lies within $\sim 30^\circ$ from the line of sight, and at an angle of $130^\circ \rightarrow 180^\circ$ (measured E from N), with very high uncertainties (see Priour et al. 2002). If we assume that the polar axis of the latitude-dependent wind lies perpendicular to the orbital plane, we would then have to place it close to the plane of the sky, and at an angle of $40^\circ \rightarrow 90^\circ$ (measured E from N). This direction for the polar axis, taken together with the direction of Mira’s proper motion (see above) implies that the polar axis of the outflow has to lie at an angle $\alpha \sim 33^\circ \rightarrow 83^\circ$ with respect to the direction of relative motion of the ISM which is streaming past Mira’s wind.

After exploring a limited set of ~ 10 parameter combinations, we have chosen a model in which the angle between the polar axis of the latitude-dependent wind and the direction of the streaming environment has a value of 70° , which is consistent with the observations described above. In §2, we describe the choice of parameters for our model, and the results from the numerical time-integration. In §3, we discuss the results.

2. THE MODEL

We model the cometary tail of Mira as the interaction of a latitude-dependent wind with a homogeneous environment in relative motion with respect to Mira. For the stellar wind, we consider a density of the form :

$$\rho(r, \theta) = \frac{A}{r^2} f(\theta), \quad f(\theta) = \xi - (\xi - 1) |\cos \theta|^p, \quad (1)$$

Electronic address: raga@nucleares.unam.mx

¹Instituto de Ciencias Nucleares, Universidad Nacional Autónoma de México, Ap. 70-543, 04510 D.F., México

²Instituto de Astronomía, Universidad Nacional Autónoma de México, Ap. 70-543, 04510 D.F., México

³Dublin Institute for Advanced Studies (DIAS), 31 Fitzwilliam Place, Dublin 2, Ireland

⁴Instituto de Geofísica, Universidad Nacional Autónoma de México, 04510 D.F., México

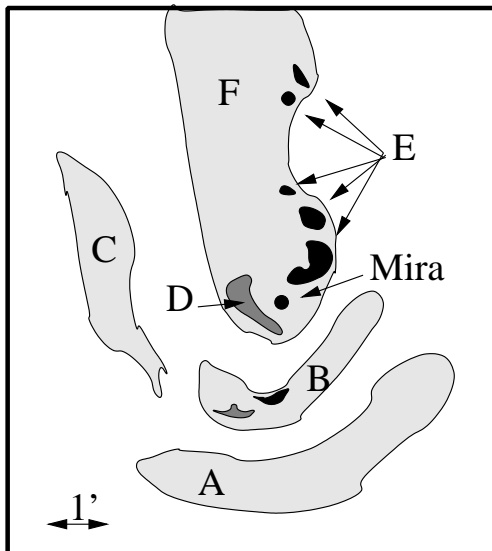


FIG. 1.— Schematic diagram of the UV image of the head of Mira’s comet, showing the structures seen in Figure 3 of Martin et al. (2007). The proper motion of Mira is directed at an angle of $\approx 7^\circ$ to the W of S (N is up and E is left), approximately aligned with the large scale structure of the cometary tail. Therefore, when comparing this diagram with the model predictions (Figures 2-4), one has to allow for this small deviation from the vertical direction of Mira’s motion. In this Figure, we introduce labels A-F in order to identify the different structures which are discussed in the text.

where r is the spherical radius and θ is the polar angle (measured out from the symmetry axis of the wind). In this equation, A is a scaling constant, $\xi > 1$ is the equator-to-pole density ratio, and p is a constant that determines the degree of flattening towards the equator of the density stratification. We have taken this form of the anisotropy function $f(\theta)$ from Riera et al. (2005).

We now consider a latitude-dependent wind velocity of the form

$$v(\theta) = \frac{v_0}{\sqrt{f(\theta)}}. \quad (2)$$

where v_0 is the velocity of the wind in the polar direction. With this choice, the ram pressure ρv^2 of the wind is isotropic.

One can relate the scaling constant A with the mass loss rate of the wind \dot{M}_w through the relation

$$\begin{aligned} \dot{M}_w &= 4\pi r^2 \int_0^{\pi/2} \rho(r, \theta) v(r, \theta) \sin \theta d\theta = \\ &= 4\pi A v_0 \int_0^{\pi/2} [f(\theta)]^{1/2} \sin \theta d\theta. \end{aligned} \quad (3)$$

We now choose an anisotropy function with $p = 1/2$. With this choice, one can compute analytically the integral in equation (3) to obtain :

$$\dot{M}_w = (4\pi A v_0) \frac{8\xi^{5/2} - 20\xi + 12}{(\xi - 1)^2}. \quad (4)$$

We now choose a $\xi = 20$ equator to pole density ratio, for which through equation 4 we obtain $A = 0.390 \dot{M}_w / (4\pi v_0)$.

To complete the parameters for our anisotropic wind we choose a polar velocity $v_0 = 10 \text{ km s}^{-1}$ and a mass loss rate $\dot{M}_w = 7.7 \times 10^{-7} M_\odot \text{ yr}^{-1}$. We set the wind temperature equal to 10^3 K at a distance $r_w = 8 \times 10^{16} \text{ cm}$

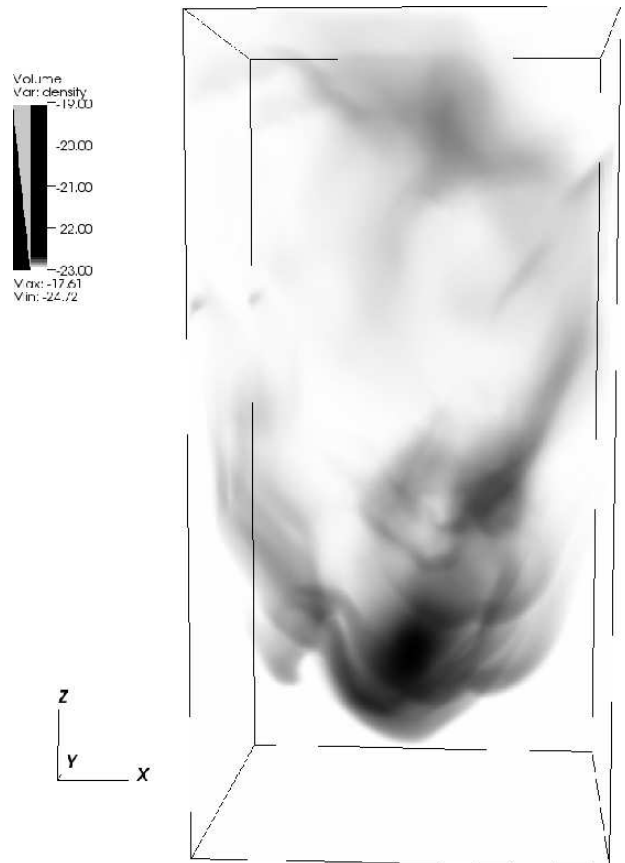


FIG. 2.— Volume rendition of the density structure obtained for a $t = 8 \times 10^4 \text{ yr}$ time integration from the simulation described in the text. The horizontal extent of the displayed domain is of $1.5 \times 10^{18} \text{ cm}$.

from the star, and impose the wind at all times within this radius. For the environment, we assume that it enters the grid along the z -axis, with a constant velocity $v_* = 130 \text{ km s}^{-1}$, density $n_{env} = 0.1 \text{ cm}^{-3}$ and temperature $T_{env} = 10^3 \text{ K}$.

Finally, we tilt the polar axis of the wind (out from which the angle θ is measured, see equations 1 and 2) so that it lies on an xz -plane, pointing at an angle $\alpha = 70^\circ$ measured from the z -axis. This angle is consistent with the orientation of the orbital axis of the Mira binary system (see §1).

We now carry out a 3D numerical simulation with the yguazú-a code in a $(1.5, 1.5, 3.0) \times 10^{18} \text{ cm}$ domain. The stellar wind source is centered on an xy -plane, and placed at a $z_0 = 6 \times 10^{17} \text{ cm}$ distance from the edge of the grid along the z -axis. This domain is resolved with a 5-level, binary adaptive grid giving $128 \times 128 \times 256$ points at the maximum resolution. The yguazú-a code has been described in detail by Raga et al. (2000), and has been tested with laboratory experiments and employed for computing many different astrophysical flows (see, e.g., the review of Raga et al. 2006). We have used the version of the code in which the gasdynamic equations are integrated together with a rate equation for the ionization of H, and uses a parametrized cooling function (computed as a function of the density, temperature and H ionization fraction), which is described by Raga & Reipurth (2004).

The numerical simulation is started with the wind (see

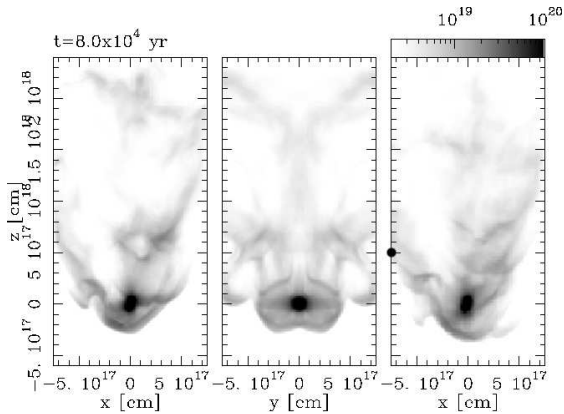


FIG. 3.— Column density maps for $t = 8 \times 10^4$ yr obtained by integrating the atom+ion column density along the y -axis (left) and along the x -axis (center). On the right we show the column density map for an orientation with the x -axis on the plane of the sky, and the z -axis at an angle $\phi = 30^\circ$ with respect to this plane. The column densities (in cm^{-2}) are shown with the logarithmic greyscale given by the bar on the top right. The origin of the coordinate system coincides with the (projected) position of the stellar wind source.

equations 1-2) occupying all of the computational domain, and the streaming environment entering from the bottom of the domain. Figure 2 shows a volume rendition of the density of the flow after a $t = 8.0 \times 10^4$ yr time-integration. The density stratification shows a leading bow shock with a complex structure, and a tail with dense clumps and filaments. Figure 3 shows the column densities obtained from this stratification, calculated by integrating the density along the y - and the x -axes, and also assuming that the z -axis is at a $\phi = 30^\circ$ angle with respect to the plane of the sky (with the x -axis on this plane). This orientation angle corresponds to the orientation of the motion of Mira with respect to the plane of the sky (see §1). The column density maps show structures with large differences depending on the direction of the integration.

In Figure 4, we show part of the time-evolution of the column density maps (calculated assuming a $\phi = 30^\circ$ angle between the z -axis and the plane of the sky) of the region around the head of the cometary structure. In this time-sequence, we see that the region upwind from the star (i. e., below the star in the frames of Figure 4) at all times has a leading thick, dense region, which corresponds to the snowplow structure of the wind/streaming ISM interaction. The projection of the 3D structure on the plane of the sky has a complex shape, at some times giving a “double bow shock” morphology (see, e.g., the $t = 7.0 \times 10^4$ yr frame of Figure 4). This leading bow shock has a general side-to-side asymmetry that resembles the observations of Mira (see Figure 1).

The separation between the star and the leading shock changes with time, giving values in the $(3.6 \rightarrow 4.2) \times 10^{17}$ cm range (measured along the projected z -axis), corresponding to $3'.8 \rightarrow 4'.4$ at the distance of Mira. An inspection of Figure 1 shows that this distance approximately corresponds to the position of condensation A.

The morphologies seen in some of the time frames of Figure 4 are remarkably similar to the head of Mira’s comet. For example, the $t = 6.5, 7.5$ and 9.0×10^4 yr frames show a “double bow” head, in which one could associate one of the bow shaped structures with conden-

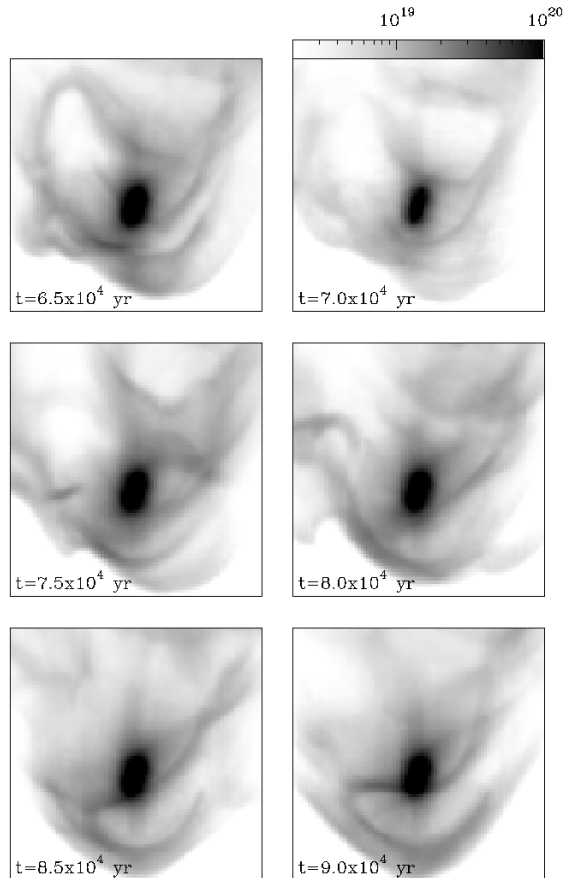


FIG. 4.— Time sequence of column density maps of the head of the cometary structure (the times in years are given on the bottom left of each of the frames). The column densities were computed for the $\phi = 30^\circ$ orientation (between the z -axis and the plane of the sky, see the text and Figure 3) of the motion of Mira. The square domains which are shown have a size of 10^{18} cm, which approximately coincides with the horizontal extent of the diagram shown in Figure 1. The column densities (in cm^{-2}) are shown with the logarithmic greyscale given by the bar on the top right.

sation A, and the other one with condensation B (see Figure 1).

In most of the time-frames shown in Figure 4, we see high density condensations in the region downstream (i. e., on top) of the star. These condensations could correspond to some of the knots labeled E in the schematic diagram of the observations of Mira’s tail (Figure 1).

The model which we are presenting produces a tail with a width of $\sim 5 \times 10^{17}$ cm (in the $\phi = 30^\circ$ column density map, see Figure 3). This width is similar to the $\sim 7'.5$ (7.2×10^{17} cm) width of Mira’s cometary tail (see Figure 1 of Martin et al. 2007).

3. CONCLUSIONS

We have presented a 3D simulation of the interaction of a tilted, latitude-dependent wind with a streaming environment. This simulation (viewed from an appropriate direction) produces column density maps which resemble the cometary structure around Mira in a qualitative way.

Our simulation produces an asymmetric leading bow shock with a structure of condensations, and also a complex, time-dependent tail (see Figure 2). If one compares the predicted column densities with the UV maps of Martin et al. (2007), one can see that the individual time-frames (Figure 4) have condensations that fall at

the approximate positions of the observed condensations (see Figure 1 and Martin et al. 2007). In particular, our model is successful at reproducing the “double bow shock” structure seen in the head of Mira’s comet, with two bow shaped condensations at approximately the correct distances away from the star.

This comparison between the predictions and the observations hinges on the the assumption that the emission coefficient of the observed emission is approximately proportional to the density, so that the features seen in the column density maps can indeed be identified with the observed, emitting condensations. This assumption is of course likely to be incorrect.

In order to advance in understanding Mira’s comet it will be essential to obtain information about the mechanisms responsible for the UV emission. Low resolution spectroscopic observations will provide information about which mechanisms produce the emission of different regions of the cometary structure. High resolution observations will provide radial velocity information, and proper motion measurements of the condensations of the cometary structure would also be possible by reimaging this object within the next few years.

The parameters of our present model are not very well constrained, except for the known spatial velocity and the orientation of Mira’s motion with respect to the surrounding medium. Also, if one assumes that the polar axis of the latitude-dependent wind is perpendicular to the orbital axis of the Mira binary system, one obtains an observational constraint for the orientation of the polar axis. We have chosen values for the mass loss rate and the wind velocity (and for the angular dependence of both of these) which are reasonable for an AGB star, and a value for the environmental density such as to give the right size for the head and tail of the cometary structure.

It is notable that through a very limited exploration (with ~ 10 attempts) of the choices for all of these parameters, one is able to obtain a model that reproduces the remarkable “double bow shock” structure of Mira’s comet. We therefore conclude that the observed double bow shock can be straightforwardly explained by a model of the interaction of a steady, latitude-dependent wind with a streaming environment, and that it is not necessary to invoke the presence of a strong time dependence in the wind in order to reproduce the observed structures. Wareing et al. (2007) arrived at a similar conclusion from their analysis of the structure of the tail of Mira’s comet.

We end our discussion by mentioning the differences between our model and the model presented by Wareing et al. (2007). The main difference between the two

models is that while Wareing et al. (2007) considered an isotropic wind, we have considered the case of a latitude-dependent wind. Another, less important difference between the two calculations is in the way the simulations were initialized.

Wareing et al. (2007) started their simulation by imposing a wind within a small, spherical region, having the rest of the computational domain filled in with a homogeneous, streaming environment. This initialization can be seen as an idealization of having a star with a wind that suddenly “turns on” as it enters its AGB phase, but it is probably not appropriate for the case of Mira (which was probably in the AGB phase before starting to interact with the ISM in the galactic plane).

We have started our simulation assuming that the stellar wind fills the computational domain, and that the streaming environment begins to enter the computational domain from one of the grid boundaries. This is an idealization of the situation in which a stellar wind source that moves through a very low density environment suddenly enters a much higher density medium (i. e., the star meets the galactic plane), which is also an idealized situation that probably does not correspond to the evolution of Mira’s comet (which has been travelling through the stratified, galactic plane ISM for a much longer time than the time-integration of our simulation).

However, we find that for integration times $> 5 \times 10^4$ yr the structures obtained in the head of the cometary structure (see, e.g., Figure 4) are qualitatively similar with both of the two initializations described above. A detailed description of the long tail of the cometary tail, however, might require a model in which the passage of Mira through a more realistic galactic plane ISM is considered.

This work was supported by the CONACyT grants 46828-F and 61547, the DGAPA (UNAM) grant IN 108207 and the “Macroproyecto de Tecnologías para la Universidad de la Información y la Computación” (Secretaría de Desarrollo Institucional de la UNAM, Programa Transdisciplinario en Investigación y Desarrollo para Facultades y Escuelas, Unidad de Apoyo a la Investigación en Facultades y Escuelas). FDC acknowledges support of the European Community’s Marie Curie Actions - Human Resource and Mobility within the JETSET (Jet Simulations, Experiments and Theory) network under contract MRTN-CT-2004 005592. We thank Enrique Palacios, Martín Cruz and Antonio Ramírez for supporting the servers in which the calculations of this paper were carried out. We also thank an anonymous referee for helpful comments.

REFERENCES

- Balick, B., Frank A. 2002, *ARA&A*, 40, 439
 Evans, D. S. 1967, in *IAU Symp. 30, Determination of Radial Velocities and Their Applications*, Ed. A. H. Batten & J. F. Heard (London: Academic Press), 57
 Knapp, G. R., Pourbaix, D., Platais, L., Jorissen, A. 2003, *A&A* 403, 993
 Martin, D. C., Seibert, M., Neill, J. D., Schiminovich, D., Forster, K., Rich, R. M., Welsh, B. Y., Madore, B. F., Wheatley, J. M., Morrissey, P., Barlow, T. A. 2007, *Nature*, 448, 780
 Raga, A. C., Navarro-González, R., Villagrán-Muniz, M. 2000, *RMxAA*, 36, 67
 Raga, A. C., Reipurth, B. 2004, *RMxAA*, 40, 15
 Raga, A. C., Velázquez, P. F., De Colle, F., Cerqueira, A., Vazconcelos, M. J., Esquivel, A., Gonzáles, R. F., Martinell, J., Herrera, J., Kajdic, P., Cantó, J., Navarro-González, R., Villagrán-Muniz, M., Sobral, H. M. 2006, *AIPC*, 875, 320
 Riera, A., Raga, A. C., Alcolea, J. 2005, *RMxAA* 41, 147
 Turon, C., et al. 1993, *Bull. Cent. Donnees Stellaires*, 43, 5
 Wareing, C. J., Zijlstra, A. A., O’Brien, T. J., Seibert, M., 2007, *ApJ*, 670, L125